

The stable isotope setting of *Australopithecus sediba* at Malapa, South Africa

AUTHORS:

Emily Holt¹

Paul Dirks^{1,2,3}

Christa Placzek¹

Lee Berger² 

AFFILIATIONS:

¹Department of Geosciences, College of Science and Engineering, James Cook University, Queensland, Australia

²Evolutionary Studies Institute, DST/NRF Centre of Excellence in Palaeosciences, University of the Witwatersrand, Johannesburg, South Africa

³School of Geosciences, University of the Witwatersrand, Johannesburg, South Africa

CORRESPONDENCE TO:

Paul Dirks

EMAIL:

paul.dirks@jcu.edu.au

POSTAL ADDRESS:

James Cook University: College of Science and Engineering, Townsville Campus, Townsville QLD 4811, Australia

DATES:

Received: 19 Oct. 2015

Revised: 10 Feb. 2016

Accepted: 12 Feb. 2016

KEYWORDS:

palaeovegetation; carbonate-cemented; cave sediments; palaeoclimate

HOW TO CITE:

Holt E, Dirks P, Placzek C, Berger L. The stable isotope setting of *Australopithecus sediba* at Malapa, South Africa. *S Afr J Sci.* 2016;112(7/8), Art. #2015-0351, 9 pages. <http://dx.doi.org/10.17159/sajs.2016/20150351>

We report $\delta^{13}\text{C}$ and $\delta^{18}\text{O}$ results from carbonate-cemented cave sediments at Malapa in South Africa. The sediments were deposited during a short-period magnetic reversal at 1.977 ± 0.003 Ma, immediately preceding deposition of Facies D sediments that contain the type fossils of *Australopithecus sediba*. Values of $\delta^{13}\text{C}$ range between -5.65 and -2.09 with an average of $-4.58 \pm 0.54\%$ (Vienna Pee Dee Belemnite, VPDB) and values of $\delta^{18}\text{O}$ range between -6.14 and -3.84 with an average of $-4.93 \pm 0.44\%$ (VPDB). Despite signs of diagenetic alteration from metastable aragonite to calcite, the Malapa isotope values are similar to those obtained in two previous studies in South Africa for the same relative time period. Broadly, the Malapa $\delta^{13}\text{C}$ values provide constraints on the palaeovegetation at Malapa. Because of the complex nature of the carbonate cements and mixed mineralogy in the samples, our estimates of vegetation type (C_4 -dominant) must be regarded as preliminary only. However, the indication of a mainly C_4 landscape is in contrast to the reported diet of *A. sediba*, and suggests a diverse environment involving both grassland and riparian woodland.

Introduction

Palaeoclimate and palaeoenvironment studies are important for identifying the drivers of hominin evolution.^{1,2} Long-term shifts and variability in climate are linked to changes in floral and faunal assemblages, which have been matched with significant points in hominin development.¹⁻³ Studies that investigate the link between climate and hominin evolution have focused on Africa because of its relatively extensive hominin fossil record, which extends back millions of years and coincides with significant palaeoenvironmental changes.²

Caves are prevalent in the Cradle of Humankind (CoH) area of South Africa. These caves are important because they contain records of changes in climate⁴ and they host hominin fossils⁵. The caves act as natural traps for floral and faunal remains, capture wind- and water-borne sediments, and are host to carbonate cave deposits.^{6,7} In a number of cave settings, fossils and sediments have been preserved in a definable stratigraphic sequence, and owing to the relatively stable nature of the cave these layers have remained undisturbed over long periods of time.⁶ Thus, CoH caves are invaluable for analysing the links between changes in climate and terrestrial environments with hominin evolution.⁸

Stable isotope proxies in carbonate cave deposits have been used to investigate late Pliocene and early Pleistocene climate and environmental conditions in South Africa.^{9,10} In the Makapansgat Valley, an area rich in hominin fossils, Hopley et al.⁹ used oxygen isotope values to time-constrain cave carbonate (flowstone) deposition at Buffalo Cave, and to determine the major orbital cycles influencing climate and vegetation patterns. In addition, the flowstone carbon isotope values and organic matter contained therein were used to ascertain changes in the dominant vegetation type (i.e. C_3 versus C_4) during the early Pleistocene. A major finding by Hopley et al.⁹ was an increase in C_4 vegetation in samples less than 2 million years (Ma) old, with the most significant increase in C_4 vegetation after 1.7 Ma.⁹ Similarly, Pickering et al.¹⁰ used carbon isotope values from cave carbonate deposits at Gladysvale Cave in the CoH. They reported a mixed C_4 -dominant CoH landscape and a cool dry environment during the early Pleistocene ($\sim 1.8 \pm 0.7$ Ma).

The ability of cave carbonates to reveal information about Plio-Pleistocene climate and vegetation has been established. However, studies from the modern summer rainfall region of South Africa are lacking. Limestone mining has displaced key stratigraphic sequences, which has led to dislocation of cave deposits and the proxies they contain, from important faunal fossils.^{9,11} Challenges in defining stratigraphy are compounded by the difficulty in forming time-depth series because of the uneven rates of sedimentation and mineral growth, and the shortage of appropriate techniques for absolute dating.^{7,12} Furthermore, in dolomitic areas such as the CoH, interpretations of oxygen and carbon isotope values from carbonates are affected by post-depositional diagenetic alteration of metastable aragonite to calcite.¹³

Despite the difficulties presented by the setting, cave carbonate studies in the CoH remain important for linking climate and environmental change with hominin evolution. Expansion of stable isotope studies to carbonate-cemented cave sediments associated with hominin fossils in the CoH provide a valuable source of information for palaeoclimate studies. In this paper, we present stable oxygen and carbon isotope data from Malapa in the CoH. The isotope data were obtained from a thin flowstone drape and carbonate cements, deposited within a cave setting in close proximity to the type fossils of *A. sediba*.^{7,14} Based on a combination of uranium-series dating and palaeomagnetic methods,^{7,14} the depositional age of the tested flowstone drape coincides with the age obtained for the *A. sediba* fossils at 1.977 ± 0.003 Ma.

We compared the raw stable isotope results with the results from studies at Gladysvale¹⁰ and Buffalo Cave⁹. Modelling was applied to the carbon isotope values in an effort to place constraints on the dominant vegetation type and past environment overlying the cave. Our results provide an initial assessment of possible vegetation conditions during the time when *A. sediba* was alive. In addition, important textural and mineralogical constraints are defined, providing guidance for future studies.

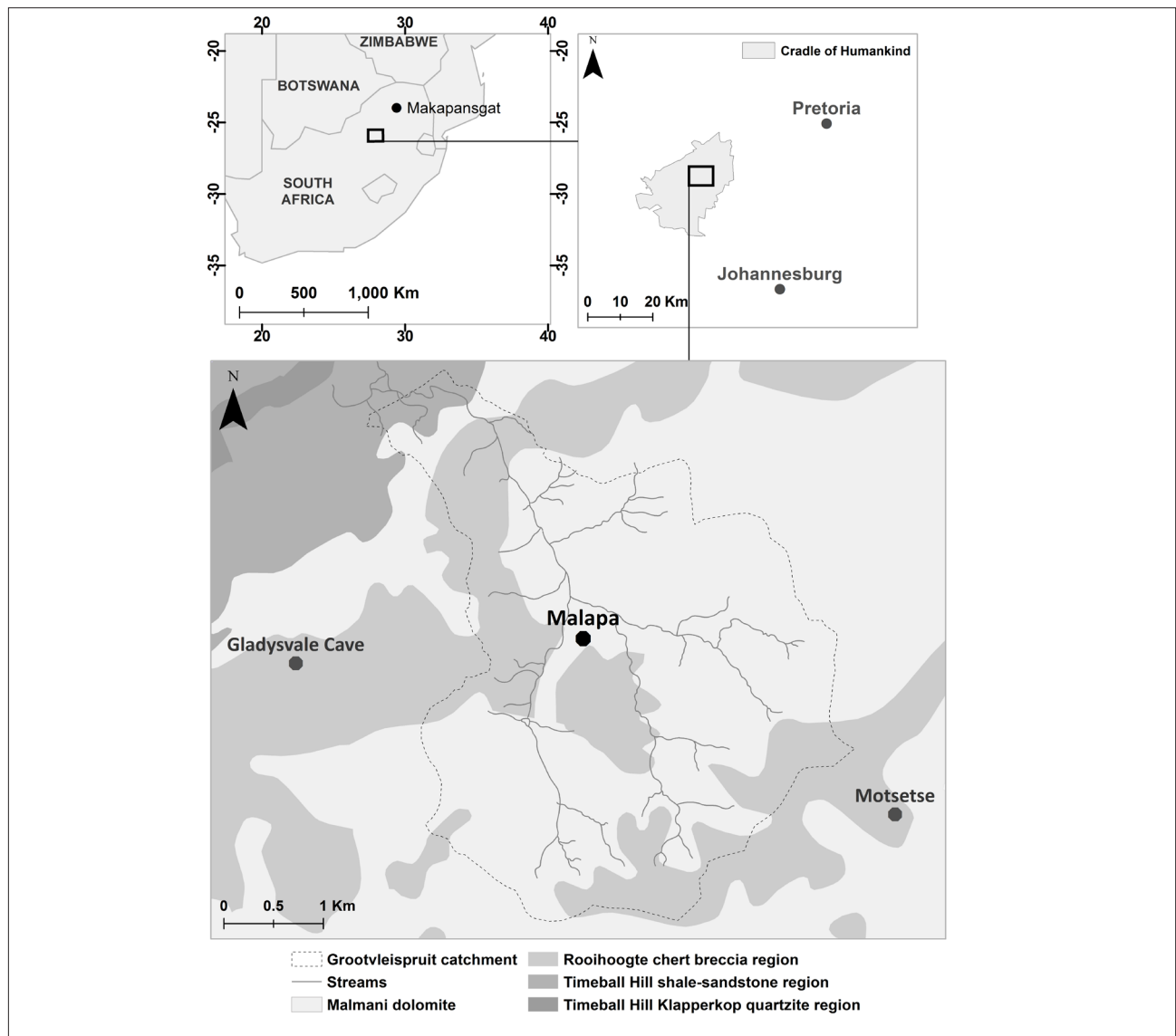


Figure 1: Location and geological setting of Malapa. Also shown is the location of another important hominin fossil site in South Africa, the Makapansgat Valley in Limpopo Province.

Site location

Malapa is located approximately 40 km northwest of Johannesburg at 25°52'S, 27°48'E (elevation 1440 masl) in the Grootvleispruit catchment, and is hosted by chert-free dolomite of the Palaeoproterozoic Lyttelton Formation in the Malmani Group (Figure 1).⁷ The site comprises two small pits excavated by miners in the early part of the 20th century.¹⁴ The larger pit, Pit 1, measures approximately 20 m² on the ground and 4 m deep, and hosts the type fossils of *A. sediba*.¹⁵ Pit 1 was the source of samples obtained in our study. A second smaller pit, Pit 2, which is roughly 12 m² in size and 1 m deep, is situated nearby and also hosts hominin remains.^{7,14}

Current climate and vegetation

Pretoria (elevation 1330 masl) is the closest monitored weather station to Malapa, and demonstrates a clear seasonal pattern in temperature and monthly rainfall. The highest temperatures occur from December to February (local summer), with February recording an average daytime temperature of 23.5 °C (1999–2013).¹⁶ July (local mid-winter) is the coldest month, with an average daytime temperature of 12.6 °C.¹⁶ The mean annual temperature (MAT) is 19.3 °C and the average annual rainfall is 700 mm, with most rain occurring in the summer months.¹⁶

Vegetation cover in the CoH is a consequence of precipitation, geology, MAT, and location within the landscape.^{17–19} Malapa is situated within the Carleton Dolomite Grassland, which is dominated by a single layer of C₄ photosynthetic process grasses.¹⁹ However, this area also has a high level of species richness because of the heterogeneous nature of the dolomitic landscape.¹⁹ A range of woodland communities occurs in specific areas,^{18,19} such as near cave entrances¹⁸ and at spring sites or along streams. In addition, C₃-type grasses are common at relatively high and cool elevations, and in areas that experience winter rainfall.^{17,19}

Depositional setting and stratigraphy

The depositional history and stratigraphy of the Malapa site has been well described.^{7,14} The type fossils of *A. sediba* (MH1 and MH2)¹⁵ were found within poorly-sorted sandstone of Facies D, which has been interpreted as a mass flow deposit.⁷ A flowstone unit from Pit 1, measuring 5 cm to 20 cm in thickness (Flowstone 1), has been dated to 2.026 ± 0.021 Ma⁷ and presents an important chronostratigraphic marker for Facies D. Flowstone 1 consists of a single sheet in the southeast corner of the pit, and splits first into two and then into three separate sheets towards the centre of the pit, where the top sheet directly underlies the *A. sediba* fossils contained in Facies D.

The three sheets of Flowstone 1 are separated by layers of fossil-bearing sandstone and siltstone, with thickness increasing from southeast to northwest.^{7,14} The basal layer of Flowstone 1 correlates with a flowstone layer in the northwest wall of Pit 1, from which the U-Pb date was obtained. This correlated flowstone records normal magnetic polarity, assigned to the Huckleberry Ridge event (~2.05–2.03 Ma) at its base, followed by intermediate polarity, and then reversed polarity. The middle and upper flowstone layers in Flowstone 1 record stable reverse polarity of the Matuyama Chron (2.03–1.95 Ma). These layers cannot be correlated with flowstone in the west wall of the pit, but thin out and disappear.⁷

Along the northwest wall of Pit 1, a finely laminated unit occurs in a lateral up-dip position from the flowstone. This laminated unit is composed of mm-scale sandstone–siltstone layers, with angular clastic fragments (mainly dolomite, chert and speleothem) intercalated with regular drapes of flowstone (0.1 mm – 1 mm thick). Stratigraphically, the laminated unit referred to in this study as ‘Facies Da’ accumulates on top of Flowstone 1 by as much as 30 cm. The top of the unit (composed of Facies Da) constitutes the base of palaeomagnetic sample UW88-PM04. Facies Da also comprises most of palaeomagnetic sample UW88-PM09.^{7,14} Thin flowstone layers in UW88-PM04 and UW-PM09 record normal polarity.^{7,14}

Overlying Facies Da sediments are other sediments that belong to the finer-grained, weakly layered topmost section of Facies D (which were originally described as Facies C).⁷ The sediments of Facies D also record intermediate and normal polarity, indicating that Facies Da and

Facies D were both deposited during a brief magnetic reversal (the Pre-Olduvai event) at 1.977 ± 0.003 Ma.¹⁴ Facies D sediments are overlain by horizontally laminated, poorly sorted muddy sandstone of Facies E, which is also fossiliferous.⁷ Along the northwest wall of Pit 1, the sediments of Facies Da, D and E overlap an erosion remnant of peloidal fine-grained muds, which remain undated and belong to Facies C.^{7,14} Textural evidence indicates that the sedimentary units composed of Facies C, Da, D and E were deposited in a water-saturated environment.⁷

Methods

Samples

As shown in Figure 2, four samples from Pit 1 were studied for stable isotope analysis: UW88-PM09 (PM09), PM09-2 (a duplicate of PM09), UW88-PM04 (PM04) and PM04-2 (a duplicate of PM04). These samples have a well-constrained age (1.977 ± 0.003 Ma), and contain thin carbonate drapes as part of Facies Da sediment, which were deposited during the same magnetic reversal recorded in Facies D immediately before deposition of the *A. sediba* fossils. Sample PM09 comprises a base of Facies C overlain by sediment of Facies Da and Facies D, and contains a thin laminated flowstone drape between Facies C and Facies Da. Sample PM09-2 is derived from the same sample block as PM09 but was set further back in the pit wall. Samples PM04 and PM04-2 represent two separate slices of the same original rock sample collected in the north wall of Pit 1,⁷ and are largely composed of Facies D sediment.

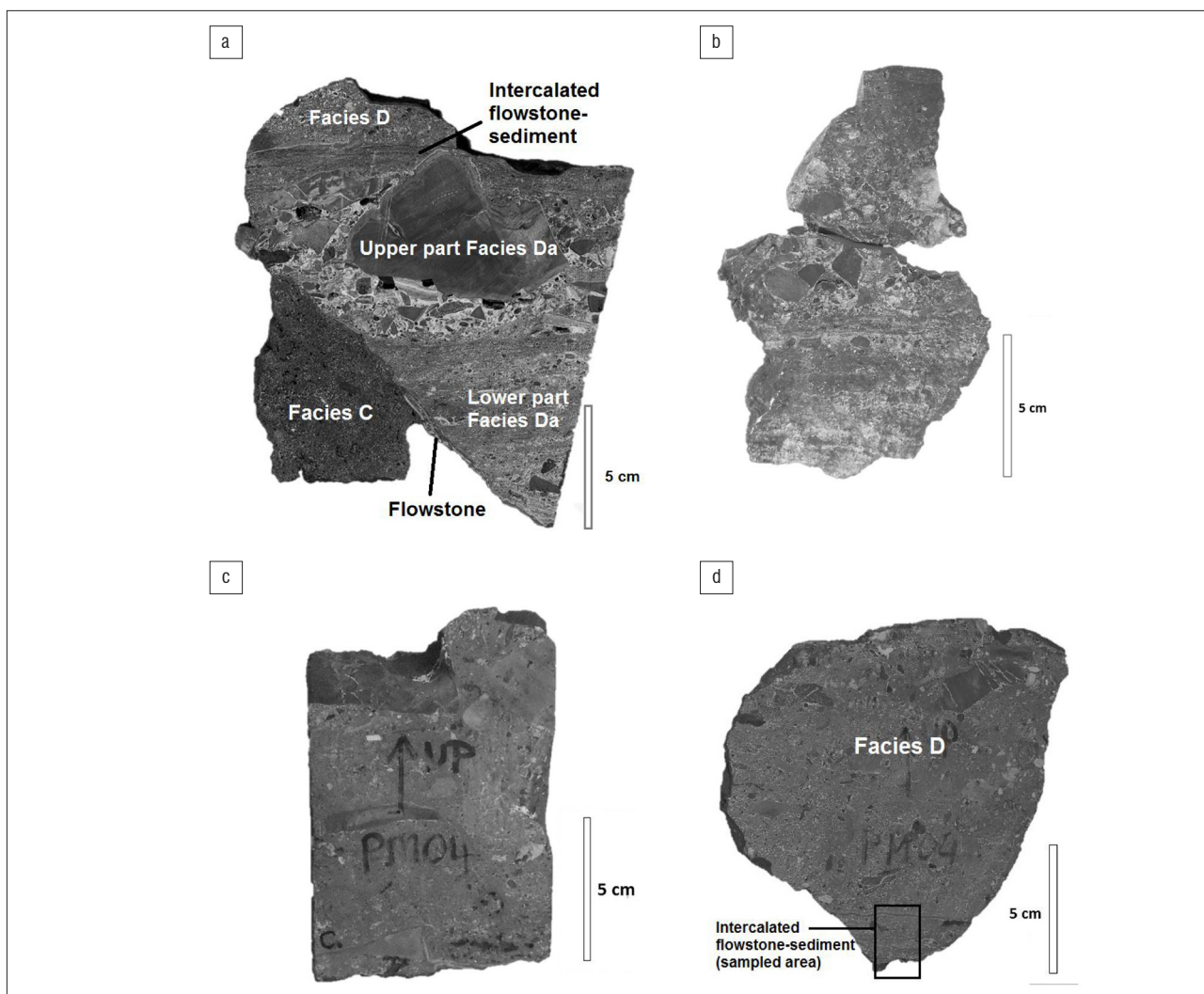


Figure 2: Malapa samples used in this study for carbonate stable isotope analysis: (a) UW88-PM09 (PM09), (b) PM09-2, (c) UW88-PM04 (PM04), (d) PM04-2. The PM09-2 is largely composed of Facies Da, whereas PM04 is largely Facies D.

The studied samples exhibit a number of relatable features, including an intercalated flowstone-sediment unit, which represents the top of Facies Da and the abrupt transition to Facies D. The inferred stratigraphic relationships between the samples indicate that they comprise a full profile of deposition that directly preceded (Facies Da) or coincided (Facies D) with the burial of *A. sediba*.

Feigl's staining of thin sections of sample PM09 revealed mixed carbonate mineralogy, evidence of post-depositional diagenesis, and a varying depositional environment (Figure 3). Evidence of primary acicular aragonite (CaCO_3) is common in all samples; however, the aragonite has largely been recrystallised to or replaced by sparry columnar calcite (CaCO_3). Thin carbonate layers in Facies Da, void fillings (laminated) in Facies Da and Facies D, and the flowstone drape separating Facies C and Facies Da show calcite-preserving relics of aragonite crystals. These crystals take various forms, including botryoidal, acicular or micrite crystals. Where aragonite relics are preserved, the diagenetic process is interpreted to be the result of calcitisation by thin water films.¹³ However, complete dissolution of primary aragonite and replacement by secondary calcite¹³ has also occurred, as evidenced by the lack of aragonite relics in parts of all facies within the samples. Crystal form confirms that Malapa was subject to fluctuating water flow and sediment input, resulting in a mixed phreatic-vadose depositional environment that was conducive to both carbonate deposition and post-depositional changes.

Sample preparation for stable isotope analysis

A total of 99 carbonate sub-samples were collected for stable isotope analysis from flowstone layers and carbonate cement within the samples described above. Samples were obtained by hand, using a standard engraving drill with removal bits measuring between 1 mm and 3 mm. Cross-contamination between sites was reduced by discarding surface material and rinsing the drill bits in 5% nitric acid, deionized water and ethanol, respectively. Carbonate powders were collected in PCR tubes, then weighed and transferred into clean glass sampling tubes.

Stable isotope analyses were performed at the Advanced Analytical Centre at the James Cook University in Cairns, Australia. The equipment used was the Thermo Scientific Delta V gas source isotope ratio mass spectrometer (IRMS) together with GasBench III and ConFlo IV interfaces. Carbonate samples were digested in 99% phosphoric acid at 25 °C, and the resulting CO_2 gas was analysed after equilibrating for 18 h. Results were normalised to Vienna Pee Dee Belemnite (VPDB) using the calibrated reference materials of NBS 19 and NBS 18, and were reported in parts per mil (‰) with delta (δ) notation. Mean analytical precision of repeat reference materials is $\pm 0.1\text{‰}$ for both $\delta^{18}\text{O}$ and $\delta^{13}\text{C}$.

Replication

Flowstones and carbonate-cemented sediments are not normally subject to Hendy criteria tests. This is because of the variable nature of growth, including difficulty in defining vertical versus lateral advances over time.²⁰ For these types of samples, replication has been suggested as a more purposeful and valuable method in stable isotope studies.²¹ In our study, sample PM09-2 was chosen for replicate analysis of the primary sample UW-PM09. The methodology for sample collection and data analysis of the replicate was the same as for the original samples.

Modelling palaeovegetation at Malapa

The values of $\delta^{18}\text{O}$ and $\delta^{13}\text{C}$ in cave deposits are governed by a complex set of variables and processes.^{22,23} Under ideal equilibrium conditions, speleothem $\delta^{18}\text{O}$ values reflect cave temperature and source water $\delta^{18}\text{O}$ values.^{22,24} The speleothem $\delta^{13}\text{C}$ values are indicative of overlying vegetation, atmospheric CO_2 and carbonate host rock-source water interaction.²⁴ However, stable isotope analysis of cave carbonates, in the context of palaeoclimate and palaeoenvironmental determinations, relies on several constraints and assumptions.^{22,24-27}

Fractionation refers to the relationship between stable isotope values in the source water (or gas) and the resulting carbonate (Equation 1).^{23,28-30}

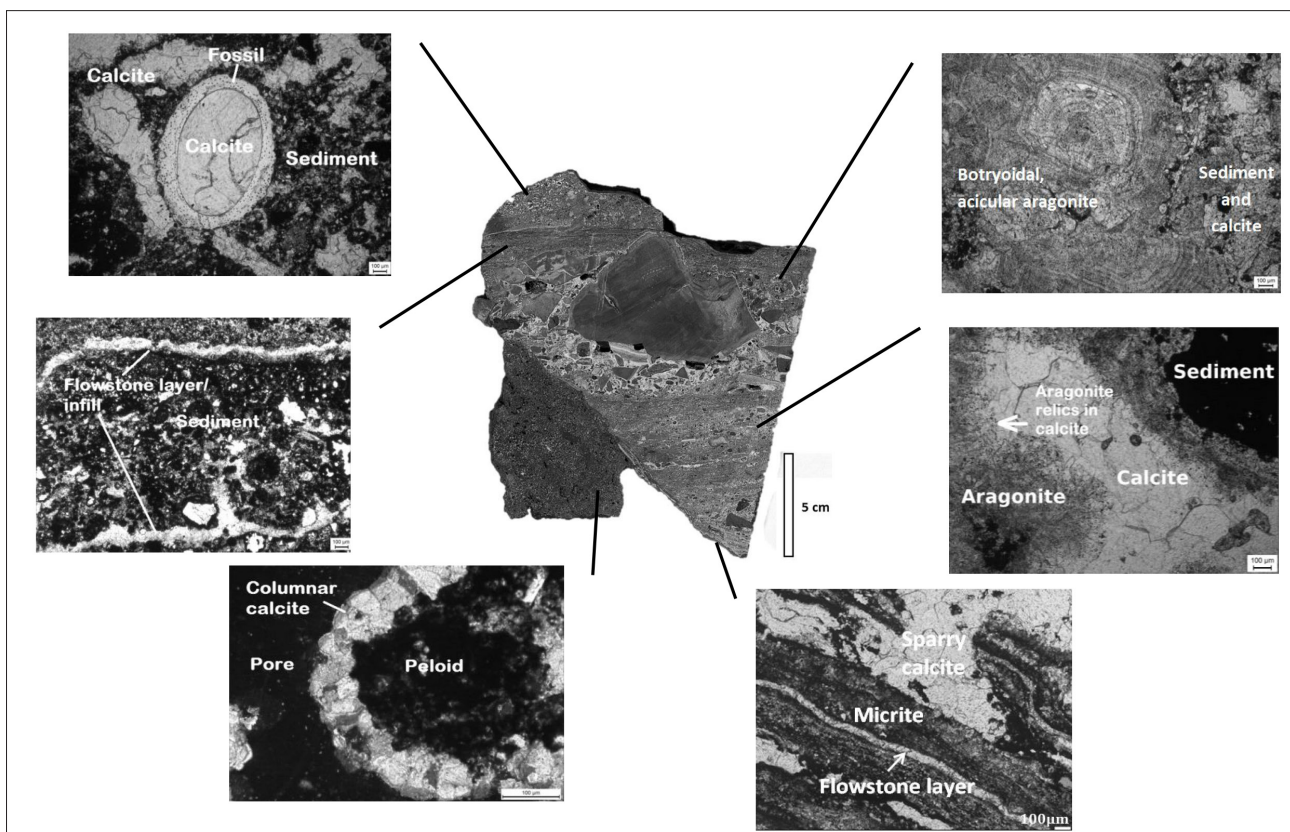


Figure 3: Thin section views from Malapa sample UW-PM09. The thin sections are shown in plane-polarised light, except Facies C which is viewed in cross-polarised light. The views illustrate a mix of carbonate mineralogy, including aragonite relics in calcite, as well as fossils and sediments.

Fractionation leads to the enrichment or depletion of the heavier isotope as phase changes (gas–liquid–solid) and reactions occur from the source to the resulting carbonate. Temperature-dependent equilibrium fractionation factors are available for carbon isotopes within cave carbonates (Equation 1).²⁸ However, the accurate application of equilibrium fractionation factors requires that either the source water or soil-gas stable isotope value, or the temperature at time of deposition must be known.^{26,31} The fractionation equation is as follows:

$$\alpha_{\text{carbonate-source}} = \frac{1000 + \delta^{18}\text{O}(\delta^{13}\text{C})_{\text{carbonate}}}{1000 + \delta^{18}\text{O}(\delta^{13}\text{C})_{\text{source}}} \quad \text{Equation 1}$$

where α (alpha) = fractionation factor, which is temperature-dependent; and the values for stable isotopes are relevant to the same standard.

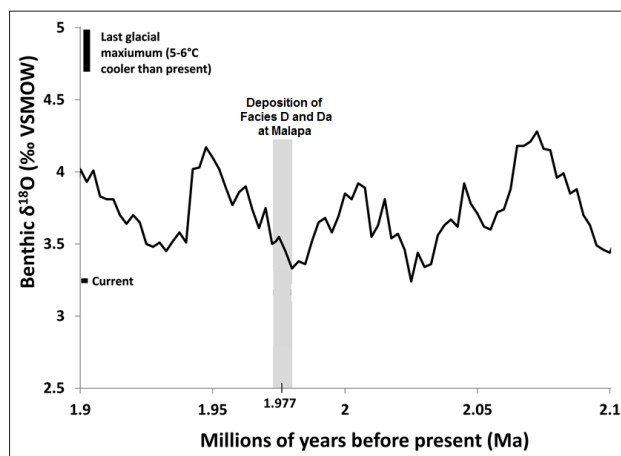
Constraining all parameters that influence stable isotope fractionation in palaeocave settings such as Malapa is not possible, if the cave environment and source-water chemistry are unknown.²⁶ Although a number of these factors, including the depositional environment, can be determined using petrographic studies and statistical analysis of stable isotope results (i.e. Hendy criteria tests for kinetic fractionation), others must be estimated. Examples of estimable factors include source-water $\delta^{13}\text{C}$ values and cave temperature. Here, we outline the estimable variables and fractionation factors used to calculate source carbon $\delta^{13}\text{C}$ values from the Malapa stable isotope values.

Fractionation factors

The primary equilibrium fractionation factors chosen for carbon source calculations in our study were those of Romanek et al.³² These factors, which include calcite- $\text{CO}_{2(\text{g})}$ and aragonite- $\text{CO}_{2(\text{g})}$ equilibrium reactions, were obtained experimentally³² and have been used in travertine studies to determine dissolved organic and inorganic carbon components.³³ In addition, we used re-evaluated factors for stepwise calcite- $\text{CO}_{2(\text{g})}$ fractionation³⁴ and back-calculated factors for step-wise aragonite- $\text{CO}_{2(\text{g})}$ fractionation.^{32,34}

Cave temperature

Cave interiors have minimal fluctuation in temperature, with cave temperature equalling surface MAT.^{21,35} Estimates of temperature at the time of cave carbonate deposition are based on known changes in MAT during glacial and interglacial periods. The minimum temperature in southern Africa during the Last Glacial Maximum (LGM) is consistent with the global temperature decrease, and has been quantified as MAT minus 6 °C.³⁶ This estimate has been obtained by analysing noble gases in groundwater.³⁶



VSMOW – Vienna Standard Mean Ocean Water

Figure 4: Change in benthic $\delta^{18}\text{O}$ during the dated Malapa time period. The benthic $\delta^{18}\text{O}$ stack of 57 globally distributed sites by Lisiecki and Raymo³⁷ shows that changes in average ocean temperature are cyclical, and could indicate global oceanic or atmospheric cooling during the Malapa sample time period.

The samples in our study were deposited within a short period of 6000 years, at 1.977 ± 0.003 Ma. During this period global temperature might have been relatively cool, as evidenced by changes in benthic $\delta^{18}\text{O}$ values (Figure 4).³⁷ Tectonic uplift and local insolation also have a bearing on MAT; however, the quantification of these effects at 1.977 ± 0.003 Ma is currently unattainable. We estimated the minimum temperature at Malapa for the studied period as having been 12.1 °C, using the current MAT (calculated as 18.1 °C)^{16,38} and the quantified minimum at the LGM. In addition, a maximum temperature of MAT minus 0.5 °C can be assumed, based on the southern African response to the LGM.³⁶

Host rock contribution to $\delta^{13}\text{C}$ values

The contribution of host rock $\delta^{13}\text{C}$ to the dissolved inorganic carbon (DIC) pool in source water can be as high as 50%, depending on various factors (e.g. source-water pH, residence time, and host rock mineralogy).^{25,30} A greater contribution of host rock $\delta^{13}\text{C}$ to the DIC pool leads to more strongly positive $\delta^{13}\text{C}$ values in the tested carbonate,²⁶ which skews the results in favour of a C_4 vegetation-dominated source. The dissolution and fractionation of dolomite, such as that which occurs at Malapa, is not well-defined. However, calcite and low magnesium calcite levels are considered to be influential components in the $\delta^{13}\text{C}$ value of source water as affected by dolomite host rock dissolution.^{27,39} For this reason, we used the calcite fractionation factor of Mook³⁴ to calculate the host rock contribution to DIC in source water, in addition to an average $\delta^{13}\text{C}$ value of -0.74‰ that was obtained from two dolomite samples at Malapa. The relative contribution of host rock dissolution to the final $\delta^{13}\text{C}$ source-water value was calculated using a simple percent contribution calculation (i.e. 10% host rock + 90% soil CO_2 = source-water $\delta^{13}\text{C}$ value).

Results

Stable isotope values

The stable isotope values for the four samples are presented in Table 1. These values demonstrated a relatively small range for $\delta^{18}\text{O}$ and a larger range for $\delta^{13}\text{C}$. For all 99 values, the mean (\pm standard deviation) $\delta^{18}\text{O}$ value was -4.93 ± 0.44 ‰, and the mean $\delta^{13}\text{C}$ value was -4.58 ± 0.68 ‰. Trends moving up the growth axis profile (i.e. from older to younger) show a statistically significant ($\alpha=0.05$) decrease in $\delta^{18}\text{O}$ values in PM09-2 (Facies Da) and the lower part of Facies Da in PM09. Replicate stable isotope results of Facies Da in UW-PM09 and PM09-2 were examined using the Welch modified 2-sample *t*-test.⁴⁰ The results confirmed that the mean values for $\delta^{18}\text{O}$ and $\delta^{13}\text{C}$ in the two samples differed significantly ($\alpha=0.05$).

Source carbon values

The calculated values of source $\delta^{13}\text{C}$ varied 1‰ according to the different estimated temperatures at deposition and the fractionation factors we used. The minimum temperature estimate (12.1 °C) yielded slightly more negative values of $\delta^{13}\text{C}$ compared with the maximum temperature estimate (17.6 °C) results. In addition, the re-evaluated fractionation factors³⁴ resulted in more strongly positive calculated $\delta^{13}\text{C}$ values compared with the experimentally obtained factors.³²

The greatest effect on calculated source $\delta^{13}\text{C}$ values was the contribution of host rock dissolution to the DIC pool. The modelling demonstrates that as the estimated host rock contribution increases from 0% to 50%, so the calculated source $\delta^{13}\text{C}$ values move towards the C_3 vegetation range (i.e. becoming more negative). This result can be explained by the model's accounting for the effect of host rock DIC on the $\delta^{13}\text{C}$ values of the tested carbonate. For a host rock contribution to the DIC pool of up to 50%, the calculated source $\delta^{13}\text{C}$ values for Malapa fit predominantly within the C_4 vegetation range (Figure 5).

Discussion

When carbonate samples are unaltered and are deposited in isotopic equilibrium with the cave environment, variations in the $\delta^{18}\text{O}$ values are linked to changes in palaeotemperature and palaeohydrology.^{30,41} The $\delta^{13}\text{C}$ values reflect the vegetation type and interaction with the host rock.^{30,41} However, the interpretation of stable isotope results from the carbonate-bearing samples of Malapa deposited at 1.977 ± 0.003 Ma is challenging.

Table 1: Stable isotope data for analysed Malapa samples

Sample and unit/facies	n	d ¹⁸ O‰ (VPDB)		d ¹³ C‰ (VPDB)	
		range	mean ± s.d.	range	mean ± s.d.
PM04 Facies D	7	-5.42 to -4.77	-5.13 ± 0.23	-4.17 to -3.89	-4.35 ± 0.26
PM04-2 Facies D	1	N/A	-5.23	N/A	-4.74
Intercalated unit (top Facies Da)	9	-6.13 to -5.17	-5.37 ± 0.30	-5.10 to -4.08	-4.73 ± 0.36
PM09-2 Facies Da	25	-5.70 to -5.10	-5.31 ± 0.14	-4.88 to -3.45	-4.26 ± 0.48
PM09 Facies D	1	N/A	-4.25	N/A	-4.80
Intercalated unit (top Facies Da)	5	-6.14 to -4.33	-4.89 ± 0.75	-5.46 to -4.62	-5.04 ± 0.33
Upper part of Facies Da	13	-5.25 to -4.25	-4.75 ± 0.27	-5.02 to -2.09	-4.29 ± 0.86
Lower part of Facies Da	33	-5.33 to -4.05	-4.65 ± 0.29	-5.65 to -4.30	-4.90 ± 0.26
All Facies Da	51	-6.14 to -4.05	-4.76 ± 0.27	-5.65 to -2.09	-4.75 ± 0.32
Flowstone drape separating Facies C ^a and Facies Da	5	-5.08 to -3.84	-4.43 ± 0.53	-5.29 to -3.55	-4.35 ± 0.72

^aFacies C is undated; therefore, results for this facies are not presented in this study

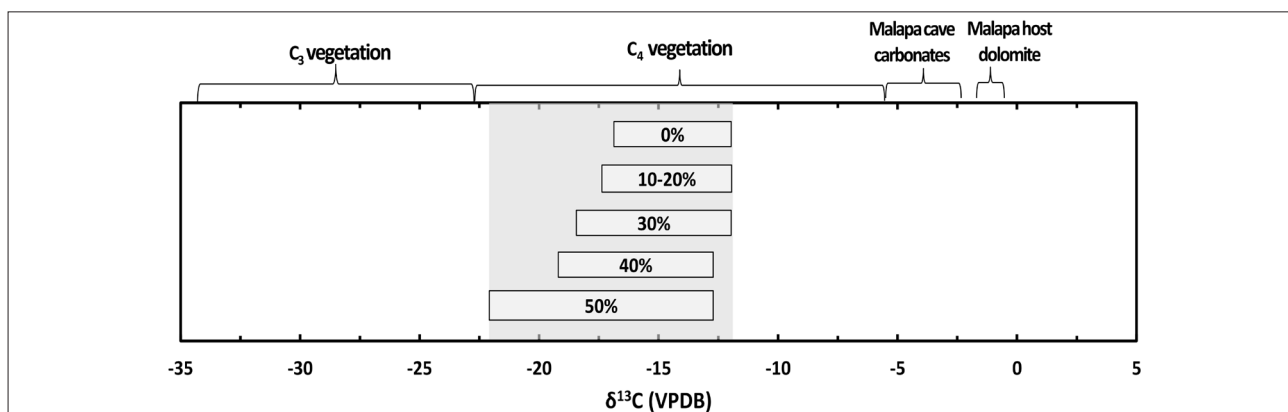


Figure 5: Calculated source $\delta^{13}\text{C}$ values for Malapa according to host rock contribution. The percentage (0%–50%) of host rock contribution to the DIC pool determines the final value of source $\delta^{13}\text{C}$. The source of carbon from vegetation overlying Malapa at 1.977 Ma is dominated by C_4 vegetation when the host rock contribution to the DIC pool is 50% or less. If a higher contribution by the host rock is assumed, results indicate a greater contribution by C_3 vegetation ($\delta^{13}\text{C}$ values for vegetation type as reported by Faure and Mensing⁴¹).

The sampled carbonates have been altered and are of mixed mineralogy, and the effect of the host rock contribution to the DIC pool is difficult to estimate. In particular, the $\delta^{18}\text{O}$ values can be markedly affected by alteration, with timing of the diagenetic event(s) difficult to define.^{42,43}

Climate change and cyclicity in Plio-Pleistocene southern Africa have been linked to, and primarily attributed to, North Atlantic sea surface temperatures and high-latitude ice volumes.⁴⁴ The Earth's orbital cycles also played a role.⁹ In particular, the influence of orbital precession on monsoonal patterns during that period is considered to have been a major driver of climate,⁹ especially prior to 2.8 Ma when 23 000-year cycles dominated.⁴⁵ The vegetation type fluctuated in response to glacial (stadial) and interglacial periods and the associated changes in rainfall and MAT, with shifts in dominant vegetation occurring rapidly.⁴⁶ Hopley⁹ suggests that after 1.7 Ma, a shift occurred towards grassland (C_4 vegetation) and away from forested landscapes (C_3 vegetation), with increasing aridity. This theory is in keeping with the change towards higher amplitude 40 000-year cycle glacial periods after 1.7 Ma.⁴⁵

The suggestion that the landscape in the region of Malapa at 1.977 ± 0.03 Ma was dominated by C_4 vegetation aligns with estimates for palaeovegetation patterns at Gladysvale Cave, albeit for the later time

of ~ 1.8 Ma (Figure 6).¹⁰ In addition, the Malapa vegetation might have been similar to the mixed C_3 -dominant vegetation in the Makapansgat Valley for the reported period, although Malapa carbonates have a more positive average $\delta^{13}\text{C}$ value.⁹ Despite difficulties in precisely correlating the timing of carbonate deposition between sites, and the effects of host rock contribution, the Malapa results could indicate that the CoH experienced a shift towards a C_4 -dominant vegetation before 1.7 Ma.

Deposition of the Malapa carbonates occurred at a time when benthic $\delta^{18}\text{O}$ values were increasing (Figure 4). An increase in the benthic $\delta^{18}\text{O}$ value indicates an increase in global ice volume, because O-16 accumulates in ice and snow⁴⁷; or it might signal cooler ocean temperatures that precede global atmospheric changes⁴⁸. Thus, a simple interpretation of benthic values during the period under study suggests that the MAT at Malapa was decreasing. However, changes in source-water $\delta^{18}\text{O}$ values, including an increase in precipitation amount, or a change in the factors affecting $\delta^{18}\text{O}$ values in precipitation (e.g. continentality, wind direction, insolation and orbital cycles) would better explain this trend. Considering the large number of variables, the data from our study were not sufficiently constrained to provide accurate palaeotemperature estimates. Nevertheless, $\delta^{18}\text{O}$ values might reflect a change in palaeohydrology.

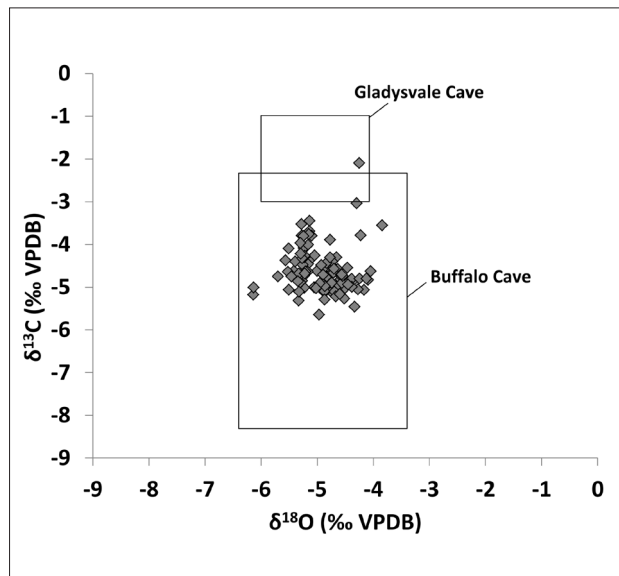


Figure 6: Comparison of stable isotope results for early Pleistocene cave carbonates in South Africa. Stable isotope results from Malapa (rhombus) are shown with reported ranges of results from Gladysvale Cave¹⁰ in the CoH and Buffalo Cave⁹ in Makapansgat Valley.

Interpretations of relative changes in aridity using $\delta^{18}\text{O}$ values in cave carbonates within the summer rainfall region of South Africa differ.^{46,49} A decrease in the $\delta^{18}\text{O}$ values of cave carbonates has been interpreted as indicating a drier climate.⁹ However, deep vertical convection, ascribed to movement of the intertropical convergence zone and subtropical highs throughout the seasonal year⁵⁰, also lead to a decrease of $\delta^{18}\text{O}$ values in precipitation and therefore also in cave carbonates. Modern data from the Global Network of Isotopes in Precipitation for Pretoria show that as rainfall and temperatures increase, the $\delta^{18}\text{O}$ value in precipitation decreases – known as the rainfall ‘amount effect’ (Figure 7).^{51–53} Furthermore, there is a strong correlation between increased rainfall in East Africa as a consequence of a positive Indian Ocean dipole, and significant depletions in $\delta^{18}\text{O}$ values in precipitation.⁵²

Implications for palaeovegetation–evolution linkages

The suggested palaeovegetation at Malapa, as reconstructed in this paper, provides an important insight into the ecological niche that *A. sediba* occupied. In studying pollen and phytolith remains recovered from plaque on teeth of *A. sediba* fossils, Henry et al.⁵⁴ found that their diet consisted wholly of leaves, fruits, the bark of trees, and herbaceous plants (C_3 vegetation). The diet of *A. sediba* is at odds with the diet of other hominin species (such as *A. africanus*)⁵⁵ in the CoH, including those from the same time period.⁵⁴ Therefore the location of Malapa, in a relatively sheltered valley near the confluence of two streams, might have provided the ideal riparian environment for *A. sediba* in an otherwise C_4 -dominated grassland.

Conclusion

Stable isotope values of cave carbonates at Malapa during the early Pleistocene are similar to those from two previous studies conducted in the summer rainfall region of South Africa. The $\delta^{13}\text{C}$ values have been used to reconstruct preliminary palaeovegetation estimates of a mixed, but possibly C_4 -dominant, landscape at 1.977 ± 0.003 Ma. Additionally, current relationships between $\delta^{18}\text{O}$ values in rainfall and rainfall amounts, and the slight decrease in the $\delta^{18}\text{O}$ values as the samples become younger, may indicate that there was an increase in rainfall and/or a change in source-water provenance during the tested time period. However, the current data are not sufficiently well constrained to derive accurate temperature estimates using $\delta^{18}\text{O}$ values, or to quantify the effect of diagenesis on $\delta^{13}\text{C}$ values. Nevertheless, carbonate-cemented cave sediments from hominin sites in the CoH are an important resource of proxies for future studies of palaeoclimate and palaeoenvironments.

Acknowledgements

We thank the South African Heritage Research Authority (SAHRA) and the Nash family for allowing us generous access to the study sites. Samples were collected under a permit granted by SAHRA (permit number 80/08/09/001/51). Funding was received by P.D. from the Australian Research Council (DP140104282), the University of the Witwatersrand, and James Cook University. We also thank the School of Geosciences and the Evolutionary Studies Institute at the University of the Witwatersrand, and the South African National Centre of Excellence in Palaeosciences, for their logistical support. Special thanks to staff and colleagues at James Cook University, especially Dr Liz Tynan for her invaluable comments on the draft manuscript.

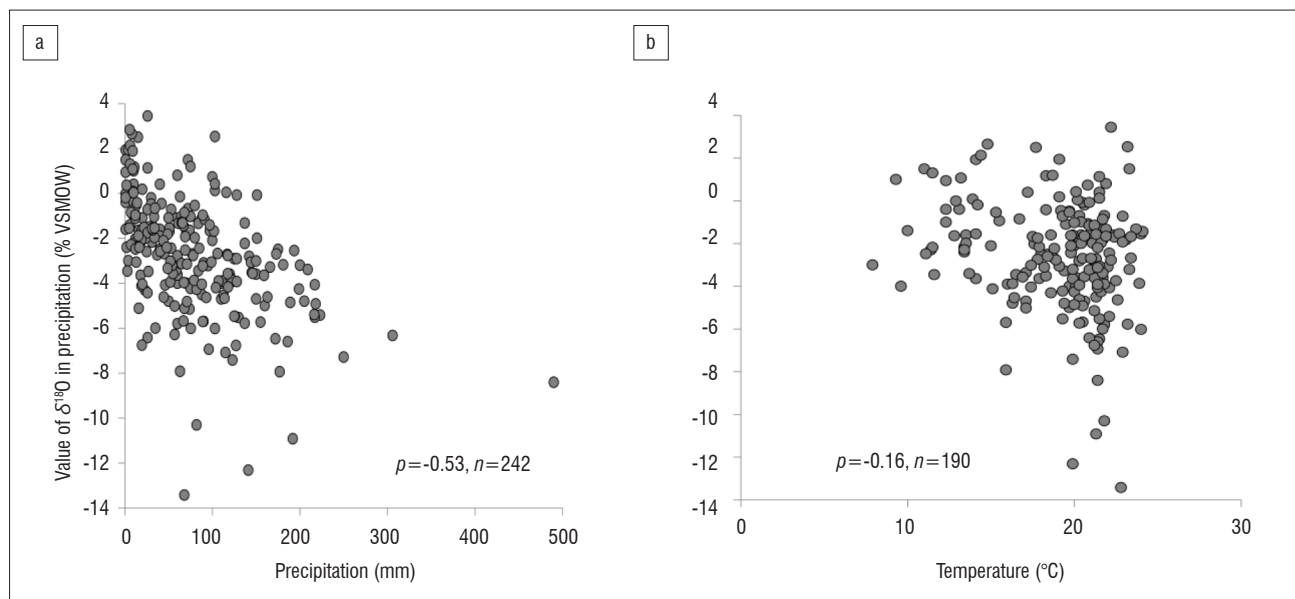


Figure 7: Oxygen isotopes in precipitation, measured for Pretoria. Monotonic relationship (Spearman’s rank correlation ρ) between reported monthly $\delta^{18}\text{O}$ values in precipitation and (a) total monthly precipitation, (b) average monthly temperatures. Both results were significant at the 95% level.

VSMOW = Vienna Standard Mean Ocean Water

Data source: IAEA/WMO⁴⁸

Authors' contributions

P.D. initiated the project, and supplied the samples. E.H. prepared the samples, performed the isotope analyses and results analysis, completed calculations for modelling, and wrote the initial version of the manuscript. P.D. contributed knowledge of the study area, commented on the interpretation of results, named 'Facies Da', and reviewed the manuscript. C.P. assisted with the modelling, provided direction for the research, and reviewed the manuscript. L.B. provided logistical support during the field component of the project, and facilitated access to the site.

References

1. deMenocal P. Climate and human evolution. *Science*. 2011;331:540–2. <http://dx.doi.org/10.1126/science.1190683>
2. Potts R. Hominin evolution in settings of strong environmental variability. *Quat Sci Rev*. 2013;73:1–13. <http://dx.doi.org/10.1016/j.quascirev.2013.04.003>
3. Vrba E. On the connections between paleoclimate and evolution. In: Vrba E, Denton G, Partridge T, Burckle L, editors. *Paleoclimate and evolution, with emphasis on human origins*. New Haven, USA and London, UK: Yale University; 1995. p. 24–45.
4. White WB. Cave sediments and paleoclimate. *J Cave Karst Stud*. 2007;69:76–93.
5. Dirks PHGM, Berger LR. Hominin-bearing caves and landscape dynamics in the Cradle of Humankind, South Africa. *J Afr Earth Sci*. 2013;78:109–31. <http://dx.doi.org/10.1016/j.jafrearsci.2012.09.012>
6. Lundelius Jr EL. Cave site contributions to vertebrate history. *Alcheringa*. 2006;30:195–210. <http://dx.doi.org/10.1080/03115510609506863>
7. Dirks PHGM, Kibii JM, Kuhn BF, Steininger C, Churchill SE, Kramers JD, et al. Geological setting and age of *Australopithecus sediba* from Southern Africa. *Science*. 2010;328:205–208. <http://dx.doi.org/10.1126/science.1184950>
8. Hopley PJ, Maslin MA. Climate-averaging of terrestrial faunas: An example from the Plio-Pleistocene of South Africa. *Paleobiology*. 2010;36:32–50. <http://dx.doi.org/10.1666/0094-8373-36.1.32>
9. Hopley PJ, Marshall JD, Weedon GP, Latham AG, Herries AIR, Kuykendall KL. Orbital forcing and the spread of C4 grasses in the late Neogene: Stable isotope evidence from South African speleothems. *J Hum Evol*. 2007;53:620–634. <http://dx.doi.org/10.1016/j.jhevol.2007.03.007>
10. Pickering R, Hancox PJ, Lee-Thorp JA, Grün R, Mortimer GE, McCulloch M, et al. Stratigraphy, U-Th chronology, and paleoenvironments at Gladysvale Cave: Insights into the climatic control of South African hominin-bearing cave deposits. *J Hum Evol*. 2007;53:602–619. <http://dx.doi.org/10.1016/j.jhevol.2007.02.005>
11. Latham AG, Herries A, Quinney P, Sinclair A, Kuykendall K. The Makapansgat Australopithecine site from a speleological perspective. *Geol Soc Sp*. 1999;165:61–77. <http://dx.doi.org/10.1144/GSL.SP.1999.165.01.05>
12. Woodhead J, Pickering R. Beyond 500 ka: progress and prospects in the U-Pb chronology of speleothems, and their application to studies in palaeoclimate, human evolution, biodiversity and tectonics. *Chem Geol*. 2012;322–323:290–299. <http://dx.doi.org/10.1016/j.chemgeo.2012.06.017>
13. Hopley PJ, Marshall JD, Latham AG. Speleothem preservation and diagenesis in South African hominin sites: Implications for paleoenvironments and geochronology. *Geoarchaeology*. 2009;24:519–547. <http://dx.doi.org/10.1002/gea.20282>
14. Pickering R, Dirks P, Jinnah Z, de Ruiter D, Churchill S, Herries A, et al. *Australopithecus sediba* at 1.977 Ma and implications for the origins of the Genus *Homo*. *Science*. 2011;333:1421–1423. <http://dx.doi.org/10.1126/science.1203697>
15. Berger LR, De Ruiter DJ, Churchill SE, Schmid P, Carlson KJ, Dirks PHGM, et al. *Australopithecus sediba*: a new species of Homo-like Australopit from South Africa. *Science*. 2010;328:195–204. <http://dx.doi.org/10.1126/science.1184944>
16. South African Weather Service. Weather data for Pretoria, South Africa. 2013.
17. SANBI(a). South African National Biodiversity Institute. Savanna biome [website page on the Internet]. [Cited 2015 May 30]. Available from: <http://www.plantzafrica.com/vegetation/savanna.htm>.
18. Eloff G. The phytosociology of the natural vegetation occurring in the Cradle of Humankind world heritage site, Gauteng, South Africa. [Thesis]. Pretoria: University of South Africa; 2010.
19. SANBI(b). South African National Biodiversity Institute. Grassland biome [website page on the Internet]. [Cited 2015 May 30]. Available from: <http://www.plantzafrica.com/vegetation/grassland.htm>.
20. Li ZH, Driese SG, Cheng H. A multiple cave deposit assessment of suitability of speleothem isotopes for reconstructing palaeo-vegetation and palaeo-temperature. *Sedimentology*. 2014;61:749–766. <http://dx.doi.org/10.1111/sed.12078>
21. Dorale J, Liu Z. Limitations of Hendy test criteria in judging the paleoclimate suitability of speleothems and the need for replication. *J Cave Karst Stud*. 2009;71:73–80.
22. Lachniet MS. Climatic and environmental controls on speleothem oxygen-isotope values. *Quat Sci Rev*. 2009;28:412–432. <http://dx.doi.org/10.1016/j.quascirev.2008.10.021>
23. McDermott F. Palaeo-climate reconstruction from stable isotope variations in speleothems: A review. *Quat Sci Rev*. 2004;23:901–918. <http://dx.doi.org/10.1016/j.quascirev.2003.06.021>
24. Mickler PJ, Banner JL, Stern L, Asmerom Y, Edwards RL, Ito E. Stable isotope variations in modern tropical speleothems: Evaluating equilibrium vs. kinetic isotope effects. *Geochim Cosmochim Acta*. 2004;68:4381–4393. <http://dx.doi.org/10.1016/j.gca.2004.02.012>
25. Clark I, Fritz P. *Environmental isotopes in hydrogeology*. USA: CRC Press; 1997.
26. Fairchild IJ, Baker A. *Speleothem science: From process to past environments*. Chichester, West Sussex UK: John Wiley & Sons Ltd; 2012. <http://dx.doi.org/10.1002/9781444361094>
27. Ford D, Williams P. *Karst hydrogeology and geomorphology*. Chichester, UK: John Wiley & Sons Ltd; 2007. <http://dx.doi.org/10.1002/9781118684986>
28. Chacko T, Deines P. Theoretical calculation of oxygen isotope fractionation factors in carbonate systems. *Geochim Cosmochim Acta*. 2008;72:3642–3660. <http://dx.doi.org/10.1016/j.gca.2008.06.001>
29. Chacko T, Mayeda TK, Clayton RN, Goldsmith JR. Oxygen and carbon isotope fractionations between CO₂ and calcite. *Geochim Cosmochim Acta*. 1991;55:2867–2882. [http://dx.doi.org/10.1016/0016-7037\(91\)90452-B](http://dx.doi.org/10.1016/0016-7037(91)90452-B)
30. Hendy CH. The isotopic geochemistry of speleothems—I. The calculation of the effects of different modes of formation on the isotopic composition of speleothems and their applicability as palaeoclimatic indicators. *Geochim Cosmochim Acta*. 1971;35:801–824. [http://dx.doi.org/10.1016/0016-7037\(71\)90127-X](http://dx.doi.org/10.1016/0016-7037(71)90127-X)
31. Daëron M, Guo W, Eiler JM, Genty D, Blamart D, Boch R, et al. ¹³C/¹⁸O clumping in speleothems: Observations from natural caves and precipitation experiments. *Geochim Cosmochim Acta*. 2011;75:3303–3317. <http://dx.doi.org/10.1016/j.gca.2010.10.032>
32. Romanek CS, Grossman EL, Morse JW. Carbon isotopic fractionation in synthetic aragonite and calcite: Effects of temperature and precipitation rate. *Geochim Cosmochim Acta*. 1992;56:419–430. [http://dx.doi.org/10.1016/0016-7037\(92\)90142-6](http://dx.doi.org/10.1016/0016-7037(92)90142-6)
33. Prado-Pérez AJ, Huertas AD, Crespo MT, Sánchez AM, Pérez Del Villar L. Late Pleistocene and Holocene mid-latitude palaeoclimatic and palaeoenvironmental reconstruction: An approach based on the isotopic record from a travertine formation in the Guadix-Baza basin, Spain. *Geol Mag*. 2013;150:602–625. <http://dx.doi.org/10.1017/S0016756812000726>
34. Mook W. *Introduction to isotope hydrology: Stable and radioactive isotopes of hydrogen, oxygen and carbon*. London: Taylor & Francis; 2006.
35. Talma AS, Vogel JC. Late Quaternary paleotemperatures derived from a speleothem from Cango Caves, Cape Province, South Africa. *Quat Res*. 1992;37:203–213. [http://dx.doi.org/10.1016/0033-5894\(92\)90082-T](http://dx.doi.org/10.1016/0033-5894(92)90082-T)
36. Stute M, Schlosser P. Atmospheric noble gases. In: Cook P, Herczeg A, editors. *Environmental tracers in subsurface hydrology*. Massachusetts, USA: Kluwer Academic Publishers; 2000. p. 349–377. http://dx.doi.org/10.1007/978-1-4615-4557-6_11

37. Lisiecki LE. A benthic $\delta^{13}\text{C}$ -based proxy for atmospheric pCO_2 over the last 1.5 Myr. *Geophys Res Lett.* 2010;37:1–5. <http://dx.doi.org/10.1029/2010GL045109>
38. Schaefli B, Hingray B, Picouet C, Musy A. Snow hydrology in mountainous regions. In: Hingray B, Picouet C, Musy A, editors. *Hydrology: A science for engineers*. USA: CRC Press; 2105. p. 274–320.
39. Johnson KR, Hu C, Belshaw NS, Henderson GM. Seasonal trace-element and stable-isotope variations in a Chinese speleothem: The potential for high-resolution paleomonsoon reconstruction. *Earth Planet Sci Lett.* 2006;244:394–407. <http://dx.doi.org/10.1016/j.epsl.2006.01.064>
40. Jones R, Gilliver R, Robson S, Edwards W. *S-Plus for the analysis of biological data*. Aitkenvale, Queensland: James Cook University Press; 2013.
41. Bar-Matthews M, Ayalon A, Kaufman A. Timing and hydrological conditions of Saproel events in the Eastern Mediterranean, as evident from speleothems, Soreq cave, Israel. *Chem Geol.* 2000;169:145–156. [http://dx.doi.org/10.1016/S0009-2541\(99\)00232-6](http://dx.doi.org/10.1016/S0009-2541(99)00232-6)
42. Perrin C, Prestimono L, Servelle G, Tilhac R, Maury M, Cabrol P. Aragonite-calcite speleothems: Identifying original and diagenetic features. *J Sediment Res.* 2014;84:245–269. <http://dx.doi.org/10.2110/jsr.2014.17>
43. Zhang H, Cai Y, Tan L, Qin S, An Z. Stable isotope composition alteration produced by the aragonite-to-calcite transformation in speleothems and implications for paleoclimate reconstructions. *Sediment Geol.* 2014;309:1–14.
44. deMenocal P, Bloemendal J. Plio-Pleistocene climatic variability in subtropical Africa and the paleoenvironment of hominid evolution: A combined data-model approach. In: Vrba E, Denton G, Partridge T, Burckle L, editors. *Paleoclimate and evolution, with emphasis on human origins*. New Haven, USA and London, UK: Yale University Press; 1995. p. 262–288.
45. deMenocal P. African climate change and faunal evolution during the Pliocene-Pleistocene. *Earth Planet Sci Lett.* 2004;220:3–24. [http://dx.doi.org/10.1016/S0012-821X\(04\)00003-2](http://dx.doi.org/10.1016/S0012-821X(04)00003-2)
46. Hopley PJ, Weedon GP, Marshall JD, Herries AIR, Latham AG, Kuykendall KL. High- and low-latitude orbital forcing of early hominin habitats in South Africa. *Earth Planet Sci Lett.* 2007;256:419–432. <http://dx.doi.org/10.1016/j.epsl.2007.01.031>
47. McClymont EL, Sosdian SM, Rosell-Melé A, Rosenthal Y. Pleistocene sea-surface temperature evolution: Early cooling, delayed glacial intensification, and implications for the mid-Pleistocene climate transition. *Earth-Science Reviews.* 2013;123:173–93. <http://dx.doi.org/10.1016/j.earscirev.2013.04.006>
48. Lisiecki LE, Raymo ME. A Pliocene-Pleistocene stack of 57 globally distributed benthic $\delta^{18}\text{O}$ records. *Paleoceanography.* 2005;20(2), Art. #PA1003, 17 pages. <http://dx.doi.org/10.1029/2004PA001071>
49. Stager JC, Ryves DB, King C, Madson J, Hazzard M, Neumann FH, et al. Late Holocene precipitation variability in the summer rainfall region of South Africa. *Quat Sci Rev.* 2013;67:105–20. <http://dx.doi.org/10.1016/j.quascirev.2013.01.022>
50. Feng X, Faiia AM, Posmentier ES. Seasonality of isotopes in precipitation: A global perspective. *J Geophys Res Atmos.* 2009;114, Art. #D08116, 12 pages. <http://dx.doi.org/10.1029/2008JD011279>
51. IAEA/WMO. Global Network of Isotopes in Precipitation: The GNIP database. 2014. [Cited 2014, December 31]. Available from: <http://www.iaea.org/water>.
52. Vuille M, Werner M, Bradley RS, Chan RY, Keimig F. Stable isotopes in East African precipitation record Indian Ocean zonal mode. *Geophys Res Lett.* 2005;32:1–5. <http://dx.doi.org/10.1029/2005GL023876>
53. Gat, J. R., Mook, W. G. and Meijer, H.: Environmental isotopes in the hydrological cycle, in: Vol. II Atmospheric Water, edited by: Mook, W., International Atomic Energy Agency, Groningen, 2000. 73 pages.
54. Henry AG, Ungar PS, Passey BH, Sponheimer M, Rossouw L, Bamford M, et al. The diet of *Australopithecus sediba*. *Nature.* 2012;486:90–93. <http://dx.doi.org/10.1038/nature11185>
55. Klein R. Stable carbon isotopes and human evolution. *Proceedings of the National Academy of Sciences.* 2013;110(26):10470–10472. <http://dx.doi.org/10.1073/pnas.1307308110>

Note: This article is accompanied by supplementary material.

